HHS Public Access

Author manuscript

Oncogene. Author manuscript; available in PMC 2016 May 05.

Published in final edited form as:

Oncogene. 2015 November 5; 34(45): 5662–5676. doi:10.1038/onc.2015.23.

Identification of 6-phosphofructo-2-kinase/fructose-2,6-bisphosphatase (PFKFB4) as a Novel Autophagy Regulator by High Content shRNA Screening

Anne M. Strohecker[1,2,8,*], **Shilpy Joshi**[1,2,*], **Richard Possemato**[3,4,5,6], **Robert T. Abraham**[7], **David M. Sabatini**[3,4,5], and **Eileen White**[1,2,9]

[1]Rutgers Cancer Institute of New Jersey, 195 Little Albany Street, New Brunswick NJ 08903

[2]Rutgers University, Department of Molecular Biology and Biochemistry, 604 Allison Road, Piscataway NJ 08854

[3]Whitehead Institute for Biomedical Research, 9 Cambridge Center, Cambridge MA 02142

[4]Broad Institute of Harvard and MIT, 7 Cambridge Center, Cambridge MA 02142

[5]MIT, Department of Biology, Cambridge, MA 02139

[6]NYU, Department of Pathology, 550 First Avenue, New York, NY 10016

[7]Pfizer, Oncology Research Unit, San Diego, CA 920167

[8]The Ohio State University, Departments of Molecular Virology, Immunology, and Medical Genetics, and Surgery 460 W 12th Avenue, Columbus OH 43210

Abstract

Deregulation of autophagy has been linked to multiple degenerative diseases and cancer, thus the identification of novel autophagy regulators for potential therapeutic intervention is important. To meet this need, we developed a high content image-based shRNA screen monitoring levels of the autophagy substrate p62/SQSTM1. We identified 186 genes whose loss caused p62 accumulation indicative of autophagy blockade, and 67 genes whose loss enhanced p62 elimination indicative of autophagy stimulation. One putative autophagy stimulator, PFKFB4, drives flux through pentose phosphate pathway. Knockdown of PFKFB4 in prostate cancer cells increased p62 and reactive oxygen species (ROS), but surprisingly increased autophagic flux. Addition of the ROS scavenger N-acetyl cysteine prevented p62 accumulation in PFKFB4-depleted cells, suggesting that the upregulation of p62 and autophagy was a response to oxidative stress caused by PFKFB4

[9]Corresponding Author is Eileen, White eileenpwhite@gmail.com, epwhite@cinj.rutgers.edu, FAX (732) 235-5795; VOICE: (732) 235-5329.

*Drs. Strohecker and Joshi contributed equally to this work

Potential Conflicts of Interest

EW is a member of the scientific advisory board of Forma Therapeutics. EW, DMS, RP, and AMS are co-inventors on a related patent application. RTA is an employee and shareholder of Pfizer, Inc.

Supplementary Information accompanying this paper is archived on the Oncogene website (http://www.nature.com/onc)

elimination. Thus, PFKFB4 suppresses oxidative stress and p62 accumulation, without which autophagy is stimulated likely as a ROS detoxification response.

Keywords

autophagy; autophagy regulators; Squestosome1/p62; shRNA screening; vesicle trafficking; kinases; PFKFB4; ROS; metabolism

Autophagy maintains protein and organelle homeostasis and enables survival in the absence of exogenous nutrients. Although active in most tissues in low levels, autophagy is dramatically induced by stress and starvation where it eliminates damaged proteins and organelles, and recycles their components into metabolic and biosynthetic pathways. Autophagy is critical to survive starvation and to prevent the toxic buildup of damaged or superfluous intracellular components (1).

Autophagy-mediated preservation of mitochondrial metabolism is exploited by tumor cells and is associated with promotion of mammary, lung, and pancreatic cancers, suggesting that autophagy-inhibiting strategies may have therapeutic efficacy in these cancer subtypes (2–12). In other settings, autophagy may suppress tumorigenesis by mitigating chronic tissue damage (13–17), leading to the general consensus that the role of autophagy in cancer is context dependent (12). Defective autophagy has been linked to neurodegenerative disorders such as Alzheimer's and Parkinson's diseases as well as liver disease, all characterized by the accumulation of toxic protein aggregates (18, 19). Autophagy prevents muscle wasting, and impaired autophagy has been implicated in various models of muscular dystrophy (20–23). Taken together, this suggests that autophagy-modulating therapies will be of great clinical interest: autophagy stimulators for neurodegenerative and degenerative musculo-skeletal disorders and perhaps also cancer prevention; and autophagy inhibitors to target a metabolic vulnerability in aggressive cancers. Although targeted small molecule modulators of autophagy are in development, the optimal targets remain unknown.

Studies assessing the functional consequences of pharmacologic inhibition of autophagy in multiple cancers employing the lysosomotropic agents and chloroquine (CQ) and hydroxychloroquine (HCQ) are underway. These inhibitors block autophagy at the terminal step of cargo degradation by interfering with lysosome function. CQ and HCQ suppress tumor growth in mouse models of cancer and in human cancer cell line xenografts, and have shown efficacy in patient-derived xenograft models alone and in combination with cancer therapeutics (9, 24–32). These results have prompted clinical trials with HCQ to block autophagy and enhance the activity of cancer therapy in refractory malignancies (33, 34). While the early findings of these trials are promising (35–40) there is an unmet need for more specific tool compounds to probe actionable targets in the autophagy pathway. The central problem lies in the fact that HCQ non-specifically interferes with lysosome function and likely has off-target effects (41). The current challenge is to identify the genes and regulatory points in the autophagy pathway that merit anti-cancer drug development.

To identify new autophagy regulators, we designed and executed a novel image-based high throughput shRNA screen based on functional elimination of the autophagy cargo receptor

and substrate p62/SQSTM1. p62 localizes to the site of autophagosome formation where it recognizes ubiquitinated cargo via its ubiquitin-binding domain (UBA) and delivers it to the autophagosome via its LC3 interaction region (LIR) domain (42–44). Importantly, p62 is an autophagy substrate that is degraded along with its cargo; thus, monitoring p62 levels can be employed as a surrogate of the functional state of autophagy in a given cell. Deletion of the essential autophagy genes *Atg5* or *Atg7* in mice leads to profound p62 accumulation, often in large aggregates (12). Screening shRNA libraries for genes that alter the ability of cells to eliminate aggregated p62 following metabolic stress and recovery is a novel approach to identify autophagy regulators upstream of the terminal substrate degradation step in the pathway. While our screen was designed to identify autophagy regulators, it is likely our candidate gene lists also contain p62 modulators, which are of interest independent of their regulation of autophagy given the importance of p62 in cancer.

p62 is a multi-functional protein that plays key roles in NFkB signaling (via TRAF6), bone remodeling (mutations in p62 are associated with Paget's disease), and cancer where its overexpression has been linked to tumorigenesis (15, 45–49). $p62^{-/-}$ mice are obesity prone and develop diabetes with age (50). More recently p62 has been linked to amino acid sensing via TORC1, controlling the localization and activity of the kinase via its interaction with TRAF6 (51, 52). Thus p62 is emerging as a nutrient sensor regulating redox balance and mTOR activation as well as autophagy.

We used the ability of cells to eliminate p62 following ischemic stress as a readout of the functional autophagy status of the cell. We identified 186 positive and 67 negative regulators of p62 accumulation from function-based libraries encompassing the protein kinome, components of the vesicle trafficking machinery, and a collection of GTPases. Our results highlight key interactions with core components of the endocytic and vesicle transport system, actin cytoskeleton, nutrient sensing and calcium signaling pathways required for functional autophagy. Metabolically relevant kinases and a subset of Rab GTPases were identified among the negative regulators of pathway. Many of these genes, particularly those of the vesicle trafficking library, are poorly annotated and this work will locate them within the context of autophagic regulation.

One of the high priority candidate genes identified by the screen, the bifunctional enzyme 6-phosphofructo-2-kinase/fructose-2,6-bisphosphatases-4, PFKFB4, was selected for further investigation. PFKFB4 belongs to a family of four rate-limiting enzymes (PFKFB 1–4) which control entry into glycolysis by regulating fructose-2,6-bisphosphate (F2,6BP) levels (53–55). We report here that PFKFB4 regulates autophagy by influencing redox balance in the cell. We also implicate the role of many new genes in the regulation of the autophagy pathway, which has the potential to inform the design of autophagy modulating therapies for cancer and other autophagy-related diseases.

RESULTS

p62 Modulator Screen to Identify Autophagy Regulators

We developed and executed a novel cell-based shRNA screen designed to capture both positive and negative regulators of autophagy at all steps upstream of substrate degradation.

This was done in a single assay using cells stably expressing a fluorescent version of the autophagy cargo receptor and substrate p62 (EGFP-p62) as a reporter of functional autophagy status (*Beclin1*$^{+/-}$; EGFP-p62 iBMK cells). The screen is predicated on the fact that p62 accumulates under stress in all cells and is eliminated by functional autophagy. In the absence of autophagy, this stress-induced accumulated p62 persists, and is more dramatic depending on the severity of the autophagy defect (i.e. cells with homozygous deletion of *Atg5* exhibit a greater impairment in p62 elimination than cells with allelic loss of *Becn1*) (15, 48). Thus monitoring the levels of p62 in cells following stress and recovery can be used as a surrogate of autophagy functionality.

We designed our autophagy screen differently from those conducted previously (56–62). Our assay employed murine immortalized epithelial cells possessing an allelic loss of the essential autophagy gene, *Becn1*, chosen over 293T or HeLa cells that are common choices for cell-based lentiviral screens, as the tumorigenic potential of the mouse epithelial cells is known and high priority candidate genes can be rapidly validated in syngeneic mouse models. Moreover, the *Becn1* heterozygous cells display a partial defect in autophagy that amplifies the p62 signal which enables the identification of both positive and negative regulators and maximizes the discovery potential of the screen.

Our assay stimulus, metabolic stress (1% oxygen, and glucose deprivation) (Fig. 1a), is highly physiologically relevant; autophagy localizes to hypoxic regions of tumors thus identifying genes capable of regulating autophagy under these conditions would be advantageous for cancer therapy(13). Importantly, our screen provides a functional readout of autophagy by measuring clearance of fluorescently tagged autophagy substrate EGFP-p62 containing aggregates during recovery, differentiating it from LC3-based screens that are limited to the detection of autophagosome formation at the initial step of autophagy activation. Thus, our assay enables the identification of autophagy modulators at both the beginning and throughout the late stages of the pathway in a single screen in addition to identifying modulators of p62 homeostasis.

We first evaluated the consequences of lentiviral infection and selection with puromycin on the elimination of p62 from autophagy competent or deficient cell lines. Although both infection and selection modestly increased baseline p62 levels in this system, EGFP-p62 accumulated in both *Becn1* wild type and heterozygote cell types under stress, and a clear difference in the ability of the autophagy-competent and -deficient cells to eliminate p62 was retained as measured by Western blot and immunofluorescence, consistent with prior studies (15) (Fig. 1a–c). Predictably, a markedly shorter timeframe of stress and recovery was needed to visualize accumulation and elimination of p62 when coupled to the additional stresses of infection and selection (7 hour stress, 18 hour recovery compared to 3 day stress, 2 day recovery) (15). A schematic of the screening protocol and representative images from the screen is provided (Fig. 1d). Three classes of candidate genes were expected: those whose expression loss restored clearance of p62 (putative negative regulators of autophagy), genes whose expression loss further impaired p62 elimination leading to an accumulation of p62 (putative positive regulators of autophagy), and genes whose expression loss had no effect on p62 elimination.

Loss of *mTOR*, the master negative regulator of autophagy, restored functional autophagy and clearance of p62 (Fig. 1d). Loss of the gene that encodes IKK-β, a known autophagy promoter (63), *Ikbkb*, resulted in significant accumulation of p62 (Fig. 1d). Those genes whose loss had no effect on p62 homeostasis, illustrated by cells infected with a hairpin targeting luciferase, constitute a third category (shRNA Control, Fig. 1d). Single cell image analysis of p62 abundance was achieved via a customized Cellomics algorithm (see methods for complete algorithm settings) (Fig. 1e). Representative images of cells infected with control shRNA (pLKO-empty T) or shRNA targeting p62 (pLKO-p62 #3) are shown with and without overlay of the algorithm.

Screen Performance

We screened more than 11,000 hairpins targeting 1361 unique genes from function-based libraries encompassing the protein kinome, components of the vesicle trafficking machinery, and a large collection of GTPases (Table S1). These gene sets were enriched in genome wide screens for autophagy regulators (56, 64) and are predicted to contain signaling as well as machinery regulators of the autophagy pathway. Genes were targeted by five to ten unique hairpins (depending on the library) and infected in quadruplicate.

Primary screen data were filtered to remove hairpins with poor infection efficiency or nuclei counts less than 1500 that likely represent autofocus errors or toxicity. The distribution of the remaining hairpins plotted against robust-z-score is shown (Fig. 2a). Negligible differences in batch-to-batch distribution of hairpins were observed, enabling analysis to be conducted on the entire screen data set at once (Fig. 2b). A non-Gaussian distribution of hits, weighted heavily toward identification of positive regulators of the autophagy pathway was observed. This distribution reflects the biology of the libraries screened (i.e. likely many positive regulators of autophagy amongst vesicle trafficking components) (Fig. 2c).

Data was analyzed by the Broad Institute's proprietary Gene-E software (65). Taking the union of the second best and weighted sum metrics, we identified 186 high priority positive and 67 negative regulators of autophagy (Tables 1–2, and Supplementary Table S1). Candidate gene lists were compared to a March 2014 build of the murine genome hosted by NCBI. Genes with a 'withdrawn' status were removed from our lists, while genes whose entry's had been updated were retained. Criteria for inclusion in the positive regulator list was a gene ranking within the top 200 'live' genes in the screen possessing two or more hairpins scoring within the top 1000 hairpins in the overall screen. This cut-off represents a 14% hit rate. We extended our criteria to capture known regulators of the pathway and maximize discovery. Negative regulators were defined as genes with two or more hairpins in the top 500 hairpins in the screen, which corresponds to a 5% hit rate.

Many known positive and negative regulators of the pathway were identified increasing our confidence in the candidate gene lists. PANTHER Gene ontology analysis of the p62 modulators revealed an equivalent distribution of candidate genes within the biological process categories between the positive and negative regulators of the pathway (Figs. 2d–e and Table S2) (66).

Candidate Positive Regulators of Autophagy

Genes whose loss was associated with further impairment of p62 elimination are putative stimulators of autophagy (Table 1). This high priority candidate gene list was enriched with genes involved in metabolism and nutrient sensing (*Ulk1, Becn1, Prkaa1, Prkaa2, Stradb, Prkag1, Mark4. Pfkfb4*), core components of the endocytosis and protein trafficking machinery (*Cav3, Rab7, Snap29, Dmn2, Ap3m2, Sec23a, Vti1b)*, interactions with the actin cytoskeleton (*Pik3cg, Arpc1a, Fgfr4, Rac3, Arpc2, Pak4, Rras2, Rac1, Araf, Hras1)* and calcium/calmodulin dependent signaling *(Camk1g, Camk4, Phkg1, Camk2g, Phkg2, Phka1, Itpka, Camkk1, Doc2b).* Intracellular calcium levels may be required for vesicle fusion events which occur at various steps within the autophagy pathway, or may lead to 5′ adenosine monophosphate-activated protein kinase (AMPK)-mediated activation of the autophagy machinery via Ca^{2+}/calmodulin-dependent kinase kinase-β (CamKKβ) (67, 68). Genes involved in Toll-like (*Pik3cg, Irak1, Irak3, Map2k3, Rac1, Mapk9, Ikbkb*) and Ephrin receptor signaling (*Epha5, Fgfr4, Epa7, Ephb6, Epha6, Ryk, Mst1r, Tie1*) were also highly enriched in our positive regulator list. Moreover, multiple MAP kinase pathway components were associated with functional autophagy in this system (*Map2k3, Araf, Mknk2, Mapk9, Map3k14, Hras1*), consistent with work from our group demonstrating that Ras transformation upregulates the autophagic machinery (8).

The endosomal sorting complexes required for transport (ESCRT) machinery sort ubiquitinated cargo into multivesicular bodies and mediate membrane fusion and abcission events within the cell. Defects in the machinery have been associated with protein aggregate accumulation and neuronal toxicity. Although the precise details of the defects remain unclear, it is suspected that these phenotypes arise from problems with vesicle docking and fusion with lysosomes. Indeed, loss of multiple ESCRT components in mouse and human cell lines is associated with an accumulation of autophagosomes and amphisomes (69, 70). Our present work confirms the involvement of the ESCRT-0 component *Hrs* in the positive regulation of autophagy noted previously (71), and additionally identifies the ESCRT-II component *Vps36*, ESCRT-III components *Chmp4B* (the homologue of *Snf7b*) and *Chmp5* (*Vps60* homologue), and *Vps4b* and *Vti1b*, components of the abcission complex, as positive regulators of autophagy.

Nucleoside diphosphate kinase B (Nme)-2 and -7 were identified as positive regulators of autophagy in our screen. Intriguingly, *Nme2* was recently noted to be required for mitophagy in a genome wide screen (58). Other intriguing regulators identified in this work are *Mark4* and *Agap3*. Mark4 is an AMPK related protein kinase recently identified in *Drosophila* as a negative regulator of mTORC1 activation via interaction with the Rag complex, preventing amino acid induction of mTOR (72). *Agap3* is an ARF family GTPase previously described to be critical for degradation of poly-glutamine containing proteins that responds to ROS-induced by poly-glutamine accumulation and leads to degradation of these aggregated proteins via ubiquitin-proteasome system (73). Its role in autophagy has yet to be described.

Candidate Negative Regulators of Autophagy

Genes whose loss enhanced p62 elimination are putative negative regulators of autophagy (Table 2). This list included known inhibitors of the autophagy pathway (*mTOR, Akt1,*

Dgka, Egfr, Mapk14), and genes involved in intracellular protein transport, particularly vesicle docking (*Scfd1, Pldn, Stxbp3a, Vps33*) and Rab GTPases (*Rab39b, Rab34, Rab7l1, Rab9*). A significant enrichment of membrane associated guanylate kinase homologues (MAGUK) was observed (*Mpp3, Dlg4, Cask, Lrguk*). These proteins share conserved SH3, PDZ, and guanylate kinase domains, and are thought to function primarily as scaffolds to cluster receptors for signaling events. Of note, CASK is known to interact with the E3 ligase Parkin, a tumor suppressor and key mediator of mitophagy via its PDZ domain (74).

Validation of Known Autophagy Regulators Identified in the Screen

A subset of candidate genes was validated to confirm on-target knockdown of expression of the gene and the scoring of the p62 phenotype. This was achieved by evaluating p62 clearance or accumulation by fluorescence (EGFP-p62) and target protein expression by Western blot following infection with two control hairpins targeting *RFP* and all of the available hairpins for the gene in question (minimum of five unique hairpins). Loss of the essential autophagy gene *Atg7*, not contained in the screen set itself but added as a proof of concept control, or the known positive regulators of the autophagy pathway *Ulk1, Becn1,* or *Prkaa1* (which encodes the alpha1 subunit of AMPKα) resulted in a significant accumulation of p62 (Fig. 3a–b). Note that the antibody used to probe AMPK recognizes both the α1 and α2 subunits, while the hairpins in this validation experiment solely target *Prkaa1*. Similarly, silencing the ESCRT-0 component *Hrs* or the late endosomal small GTPase *Rab7*, known to be required for proper fusion of the autophagosome with the lysosome (75–77), resulted in a failure to eliminate p62 during recovery, confirming the need for these genes for functional autophagy. Elongation of the immature autophagosome depends on two ubiquitin-like conjugation systems that cleave and conjugate LC3 with phosphatidylethanolamine that is required for autophagosome maturation closure. We identified genes needed for phosphatidyl ethanolamine (PE) biosynthesis, ethananolamine kinase 1 and 2 (*Etnk1*, *Etnk2*) (Table 2 and Fig. 3b) as essential components for functional autophagy.

The bi-functional enzyme PFKFB4 was among the highest scoring genes that inhibited p62 elimination in our screen; found in the top 20 of all screened genes with two or more scoring hairpins in both weighted sum and second best metrics, a ranking shared by the well known autophagy regulators *Ulk1* and *Prkaa2*. The strength of this hit, coupled with the growing list of PFKFBs as druggable cancer targets and emerging evidence of increased expression of PFKFB4 in multiple solid tumor types including breast, colon, and prostate led us to select PFKFB4 for further validation (78–81) (Table 1).

PFKFB4 deficiency could have two consequences in terms of autophagy (Fig. 4a). Depletion of the enzyme could lead to increased glycolytic flux, ATP generation, activation of mammalian target of rapamycin (mTOR), and autophagy inhibition. Alternatively, PFKFB4 deficiency could lead to decreased flux into the PPP, compromising NADPH generation, leading to enhanced ROS levels sufficient to induce autophagy.

Validation of PFKFB4 as an Autophagy Regulator

As PFKFB4 has been reported to be essential for survival of multiple cancer types (78, 82, 83), we speculated that lentiviral-mediated stable knockdown would be problematic, and moved into a transient silencing system. To confirm the original screening result in this second system, we transiently silenced expression of PKFBF4 in the *Beclin1*$^{+/-}$; EGFP-p62 iBMK cells using Dharmacon Smartpool siRNAs. An experimental timeline is provided (Fig 4b). PFKFB4 knockdown was associated with EGFP-p62 accumulation, impaired cell growth, and significantly decreased viability (approx. 50% reduction) (Fig. 4c) in agreement with published reports that PFKFB4 is essential for cancer cell survival (78, 82, 83). Moreover, PFKFB4 knockdown induced robust EGFP-p62 accumulation as measured by fluorescence microscopy and western blotting (Fig. 4c and d). Surprisingly, despite inducing p62 accumulation, PFKFB4 silencing led to increased processing of microtubule-associated protein I (LC3-I) to LC3-II indicative of increased autophagic flux (Fig. 4c).

Conventionally, p62 accumulation is associated with autophagy inhibition whereas conversion of LC3-I to LC3-II is associated with autophagy induction. However, LC3-II can also accumulate due to uncleared autophagosomes secondary to inhibition of or defects in lysosomal function. To more precisely define the role of PFKFB4 in autophagy, we performed flux analysis of *Beclin1*$^{+/-}$; iBMKs stably expressing tandem-tagged ptf-LC3 (RFP-GFP-LC3). This assay enables the differential identification of autophagosomes (visualized as yellow puncta, the merge of both RFP and GFP fluorescence) and autolysosomes, (visualized by red puncta due to quenching of GFP signal in the acidic environment of the lysosomes) in a single assay (84, 85). The total number of LC3 puncta (yellow and red) in PFKFB4-depleted cells per field was almost double that of the control cells, indicative of increased autophagy flux (Fig. 4e). We confirmed this result with a pharmacologic inhibitor of lysosomal acidification, Bafilomycin A1(BA1) (86). In agreement with the tandem-tagged LC3 results, BA1 further increased LC3 puncta upon Pfkfb4 knockdown indicating that the increased number of autophagosomes was due to autophagy induction (Fig. 4e).

Having established that PFKFB4 depletion induces autophagy in *Beclin1*$^{+/-}$ iBMKs, we turned our attention to identification of the underlying mechanism. We hypothesized that PFKFB4 depletion could lead to autophagy induction by generating ROS. Therefore we investigated whether PFKFB4 knockdown altered ROS levels by flow cytometry. Peaks were well separated and the peak for PFKFB4-depleted cells showed a forward shift when compared to control peak indicative of increased ROS levels (Fig. 4f). Supplementation of PFKFB4 knockdown cells with 1mM N-Acetyl Cysteine (NAC) during transfection, shifted the peak backward, demonstrating scavenging of ROS. This observation is consistent with reports that PFKFB4 knockdown leads to ROS generation in prostate cancer cells (78). Taken together, loss of PFKFB4 increases cellular ROS levels, autophagic flux, and p62 accumulation.

PFKFB4 Inhibits Autophagy

To determine if PFKFB4 acts upstream or downstream of the essential autophagy gene Atg7 in the pathway, knockdown experiments were carried out in an isogenic pair of autophagy-

competent and –deficient tumor derived cell lines (TDCLs) (*K-Ras*$^{G12D/+}$; *p53*$^{-/-}$; *Atg7*$^{+/+}$ and *K-Ras*$^{G12D/+}$; *p53*$^{-/-}$; *Atg7*$^{-/-}$) (3). ATG7 converts LC3-I to LC3-II, enabling autophagosome formation. Twenty-four hours post-PFKFB4 knockdown, cells were exposed to ischemic conditions in order to evaluate PFKFB4 function under autophagy-inducing conditions. BA1 was used to assess autophagic flux as depicted in the experimental timeline (Fig. 5a). PFKFB4 expression was dramatically reduced in TDCLs at both 1 and 2 days post-transfection while p62 accumulation and increased LC3-II levels were observed 2 days post-transfection (Fig. 5b and c). Of note, ischemia led to accumulation of p62 that was further enhanced by PFKFB4 depletion (Fig. 5b and c). Moreover treatment with BA1 led to increased accumulation of p62 in PFKFB4-depleted cells suggestive of enhanced flux through the pathway. Similarly, LC3-I and LC3-II levels were reduced in PFKFB4-depleted cells by day 2, but were rescued by blocking flux with BA1, suggesting that the low levels of LC3 in PFKFB4-depleted cells were due to increased turnover resulting from increased autophagy flux. Under ischemia, PFKFB4 silencing led to increased processing of LC3-I to LC3-II, evidence of increased flux relative to controls. PFKFB4 knockdown in autophagy-deficient TDCLs that lack conversion of LC3-I to LC3-II also increased p62 accumulation in ischemic conditions and had similar accumulation of p62 and LC3-I independent of BA1 treatment (Fig. 5c). This suggests that PFKFB4 depletion acts upstream of ATG7 consistent with increased oxidative stress that induces autophagy and p62 upregulation.

Phase contrast images of TDCLs 2 days post-transfection with siPfkfb4 revealed that PFKFB4 depletion impaired cell growth that was further impaired by ischemia, irrespective of *Atg7* status (Fig. 5d and e). Importantly, growth was more impaired in *Atg7*$^{-/-}$ than *Atg7*$^{+/+}$ TDCLs, which might be due to greater impairment of redox balance in the absence of autophagy although viability was not significantly altered (Fig. 5d and e). To further study the impact of PFKFB4 depletion on autophagy flux in TDCLs, we generated autophagy-competent TDCLs (*K-Ras*$^{G12D/+}$; *p53*$^{-/-}$; *Atg7*$^{+/+}$) stably expressing the ptf-LC3 reporter and performed an autophagy flux assay in the presence or absence of BA1. PFKFB4 knockdown significantly increased autophagy flux, confirming the autophagy suppressive function of PFKFB4 in a second experimental system (Fig. 5f).

To directly test our hypothesis that PFKFB4 depletion leads to autophagy induction by generating ROS, we measured ROS levels by flow cytometry. We observed increased basal ROS in autophagy-deficient TDCLs likely due to autophagy deficiency compromising ROS detoxification (87). In both autophagy-competent and -deficient TDCLs, PFKFB4 depletion generated ROS that was efficiently scavenged by NAC (Fig. 5g and h).

PFKFB4 Suppresses Autophagy and p62 Accumulation by Mitigating ROS

PFKFB4 has been reported to be essential for the survival of prostate cancer cells (78). Given the physiological relevance of PFKFB4 in prostate cancer, we investigated its role in the negative regulation of autophagy in the human prostate cancer cell line PC3. An experimental timeline for studies in this system is provided (Fig. 6a). We first examined the consequences of PFKFB4 depletion on p62 accumulation and LC3-I to LC3-II conversion. Analysis of cell lysates revealed that PFKFB4 knockdown induced p62 and accumulation of both LC3-I and -II (Fig. 6b).

Phase contrast images and viability assays at 3 days post-transfection demonstrated that PFKFB4 silencing significantly impaired cell growth and viability in PC3 cells (Fig. 6b), consistent with data from the iBMK cells (Fig. 4c) and that of Ros and coworkers (78). We next measured autophagy flux in PC3 cells stably expressing the tandem tagged ptf-LC3 in the absence and presence of BA1 following PFKFB4 knockdown. Consistent with PFKFB4 deficiency promoting autophagy, increased accumulation of p62 and LC3-II were observed by western blot in cells treated with BA1 (Fig. 6c). Fluorescence images and quantitation of total LC3 puncta revealed significantly enhanced autophagy flux associated with PFKFB4 silencing (Fig. 6c). Importantly, PFKFB4 depletion led to increased ROS levels that could be quenched by NAC supplementation (Fig. 6d). Thus, PFKFB4 depletion led to accumulation of p62, stimulation of autophagic flux, ROS generation in PC3 cells.

ROS activation can lead to autophagy induction (88–90) as well as transcriptional upregulation of p62 as an anti-oxidant defense mechanism (91). If elevated ROS levels were driving p62 accumulation and autophagic flux in the PFKFB4-depleted cells, we postulated that the enhanced p62 accumulation and autophagy flux following PFKFB4 depletion should be rescued by treatment with NAC. To directly test this hypothesis, autophagy flux was analyzed in tandem tagged-LC3-expressing PC3 cells following PFKFB4 knockdown in the presence or absence of NAC. Consistent with our hypothesis, NAC supplementation at the time of transfection significantly decreased both p62 levels and autophagy flux (Fig. 6e). Western blot analysis of PC3 cells revealed a profound decrease in p62 and LC3 levels upon NAC supplementation in PFKFB4-depleted cells. Importantly, NAC supplementation led to a significant decrease in autophagy flux as evident by the quantitation of LC3 puncta in PFKFB4-deficient cells (Fig. 6e). Taken together, our data demonstrate that PFKFB4 inhibits autophagy by mitigating ROS levels, which prevents induction of p62 due to oxidative stress (Fig. 6f).

Discussion

Using a novel cell-based assay that measures the ability of cells to eliminate the autophagy substrate p62 and loss-of-function screening, we have identified candidate genes whose expression regulates autophagy either positively or negatively. A unique feature of this screen is the use of accumulation of an autophagy substrate as a readout of the culmination of autophagy rather than the number of LC3 puncta to monitor autophagy initiation (56–62). This approach enabled us to identify autophagy regulators throughout the autophagy pathway as well as modulators of p62 itself.

Our screen employed exogenously expressed p62 as a reporter. We demonstrated that autophagy competent *beclin1*$^{+/+}$ cells efficiently eliminate accumulated EGFP-p62 during recovery in full media but this clearance is blocked in autophagy impaired *beclin1*$^{+/-}$ derived cell lines (Fig. 1b–c). It is this differential elimination of p62 that is the basis of the screen. Importantly, we have previously published similar differential clearance of endogenous p62 for this cell line (as well as in *atg5*$^{-/-}$ derived iBMKs) indicating that our overexpression approach faithfully recapitulates the failed elimination of p62 in the autophagy deficient setting (15). In agreement with this work, the Mizushima lab has

recently shown that endogenous and exogenously driven p62 levels decrease similarly during productive autophagy (92).

Another unique aspect of this work is the focus on cellular GTPases and vesicle trafficking components as potential autophagy regulators. Targeting the vesicle trafficking machinery may be a means to limit kinase activity or complex formation essential for autophagy initiation. It is well known that spatio-temporal dynamics are involved at multiple levels within the autophagy cargo loading, and vesicle fusion and docking processes. This work extends our understanding of the machinery involved in autophagosome maturation and fusion as well as regulation of the pathway by the protein kinome.

Our candidate gene lists identify potential drug targets for autophagy-modulating therapies. As both activation and suppression of the pathway are therapeutically desirable outcomes, this work is an important resource. A small subset of autophagy regulators identified here scored in recent genome wide screens employing GFP-LC3 reporters. Importantly, these screens differed in their method of silencing and library source (Dharmacon siGENOME) from this assay, as well as autophagy stimulus: one screen measured regulation of basal autophagy in normal growth conditions in the H4 neuronal cell line (56), another assayed autophagy induced by Sinbis virus infection in HeLa cells (58), while a third group identified regulators of starvation-induced autophagy in human embryonic kidney 293T cells (64). Although there are many reasons candidate genes may not appear in various screens, attention should be paid to those regulators that emerge irrespective of cell type, mechanism of silencing, reporter system, or the cellular stress used to activate the pathway. These genes include *Epha6*, *Grk6*, *Gtpbp4*, *Irak3*, *Pldn*, *Prkaa2*, *Prkcz*, *Tpr*, *Shpk*, *Tlk2*, *Rab7*, *Nme2*, and *Eif2ak1*.

In this work we identify PFKFB4 as a novel autophagy regulator. PFKFB4 depletion impairs the growth and survival of cancer cells, enhances ROS levels, and profoundly induces autophagy. We demonstrate that the induction of autophagy by PFKFB4 depletion is the consequence of ROS generation, as scavenging ROS in PFKFB4 depleted cells prevented autophagy induction. PFKFB4 depletion in multiple human prostate cancer cell lines has been reported to increase ROS levels by decreasing flux through the pentose phosphate pathway which compromises NADPH production essential for scavenging of intracellular ROS (78). Interestingly, PFKFB4 silencing led to p62 accumulation despite inducing autophagic flux. These seemingly paradoxical findings can be explained by induction of p62 from oxidative stress via Nrf2 binding to the anti-oxidant response element (ARE) containing cis-element of p62 (91); supported by our observation that the addition of NAC to PC3 cells prevented accumulation of endogenous p62 in PFKFB4 depleted cells (Fig. 6e). p62 contributes to the activation of NRF2 target genes in response to oxidative stress via binding and inactivating the negative regulator of NRF2, KEAP1 (91).

Of note, *Pfkfb4* also scored on our negative regulator list. However, a July 2014 query of the TRC library revealed that the two hairpins which scored as negative regulators of autophagy and are predicted to have a 100% match to *Pfkfb4* are also predicted to have an 80% match to the well known autophagy inhibitor *Rheb*. Thus, it is possible that the ranking of PFKFB4 as a negative regulator may be attributed to off-target effects of these hairpins on *Rheb*, a

critical component of the mTOR signaling casacade. However, because RHEB levels were not interrogated and these hairpins were predicted to have significant efficacy against *Pfkfb4* itself we did not remove this gene from Table2. Importantly, the hairpins targeting *Pfkfb4* that resulted in p62 accumulation in our screen are not predicted to target *Rheb*. Critically, a second system, Dharmacon siGENOME Smartpools (made of four distinct siRNAs targeting *Pfkfb4*) supports our finding that silencing *Pfkfb4* results in robust accumulation of p62. Further, we note that the increased accumulation of p62 observed post-silencing was associated with the well-documented decrease in viability reported with loss of PFKFB4.

While this study is the first to describe PFKFB4 as an autophagy regulator, a related family member, PFKFB3 has been linked to the pathway. In rheumatoid arthritis T lymphocytes, PFKFB3 acts as an autophagy inducer (93, 94) yet in colon adenocarcinoma cells it promotes glucose uptake that suppresses autophagy by activating mTOR (95). TIGAR, a p53-inducible protein with fructose-2,6-bisphosphatase enzymatic activity identical to PFKFB4, has a similar role in suppression of cellular ROS levels and also suppresses autophagy (96, 97). Thus, it is clear that these key metabolic enzymes tightly regulate autophagy via multiple mechanisms in a context-dependent manner. Additional knowledge gained about PFKFB4 will be of value to the scientific community as PFKFB3 and PFKFB4 are emerging therapeutic targets for cancer(79, 81, 95).

In this work we have shown that PFKFB4 suppresses autophagy and p62 by mitigating oxidative stress. Although it is known that PFKFB4 promotes pentose phosphate pathway flux and NADPH production critical for antioxidant defense, our work establishes for the first time that this activity also suppresses p62 induction and autophagy. Importantly, loss of PFKFB4 promotes oxidative stress, triggering autophagy as a stress-adaptive survival mechanism.

Methods

Cell lines and reagents

Isogenic *Beclin1*$^{+/+}$ and *Beclin1*$^{+/-}$ iBMK cell lines expressing EGFP-p62 were established (13) and maintained in DMEM (Invitrogen) containing 10% fetal bovine serum (FBS) and 1% Penicillin-Streptomycin (Invitrogen). *K-Ras* ^{G12D}*; p53*$^{-/-}$; Atg7$^{+/+}$ and *Atg7*$^{-/-}$ tumor derived cell lines (TDCLs) generated from 8 week old lung tumors (3) were cultured in RPMI-1640 medium containing 10% FBS, 1% Penicillin-Streptomycin, (Invitrogen), and 1mM sodium bicarbonate (Invitrogen). The human prostate cancer cell line PC3 (ATCC CRL-1435) was maintained in RPMI-1640 medium containing 10% FBS, 1% Penicillin-Streptomycin (Invitrogen). Glucose-free RPMI-1640 or DMEM for ischemia were obtained from Invitrogen.

The following reagents were used according to manufacturer's instructions: Baflomycin A1 (Sigma-Aldrich, # B1793) CellRox Deep Red Reagent (Invitrogen, # C10422) N-acetyl Cysteine (NAC, Sigma-Aldrich, A9165), Prolong-Anti-Fade Gold mounting media (Invitrogen P10144), Hoechst 33342 (Invitrogen, #H1399), Puromycin (Sigma-Aldrich, #P8833), and chloromethyl derivative of 2′,7′-dichlorodihydrofluorescein diacetate (CM-H_2DCFDA, Invitrogen, C6827).

Antibodies

The following antibodies were used: LC3 (Novus Biologicals # NB600-1384), p62 (8), Actin (Sigma # A1978), Atg7 (Sigma # A2856), AMPKα Cell Signaling #2532), Etnk1 (Santa Cruz Biotechnology sc-13-754), Hrs (Santa Cruz Biotechnology #sc-23791), IKKβ(Cell Signaling #2370), mTOR (Cell Signaling #2972), Rab7 (Cell Signaling #2094), ULK1 (Sigma #A7481). A rabbit polyclonal antibody against PFKFB4 was developed in conjunction with Cocalico Biologicals (details in Supplemental methods).

Autophagic Flux Assay

Cells stably expressing ptf-LC3 were analyzed for autophagic flux under normal and PFKFB4 depleted conditions. Three fields (containing a minimum of 50 cells) were scored for total number of puncta (red and yellow) per condition. Nuclei were counterstained with DAPI. Where indicated, BA1 was included as a positive control for flux blockade (3nM for iBMKs and TDCLs and 10nM for PC3).

ROS measurements by Flow Cytometry

5μM Cell Rox and 10μM CM-H_2DCFDA were added to cells (in HBSS for DCFDA) for 30min at 37°C followed by measurement of mean fluorescence by flow-cytometry (FC500; Beckman Coulter, Indianapolis IN). Three independent experiments were performed analyzing 10,000 (iBMK and PC3 cells) and 5000 (K-Ras-TDCLs) cells in each experiment. NAC rescue was performed at 1mM (iBMKs and TDCLs) or 2.5mM (PC3 cell line) final concentration.

Supplementary Material

Refer to Web version on PubMed Central for supplementary material.

Acknowledgments

Grant support

This work was supported by NIH grants R37 CA53370, RC1 CA147961, R01 CA163591, R01 CA130893, the Rutgers Cancer Institute of New Jersey (P30 CA072720), Johnson & Johnson, and a gift to DMS and EW from Pfizer. AMS and SJ were supported by postdoctoral fellowships from the New Jersey Commission on Cancer Research (09-2406-CCR-E0 to AMS, DFHS13PPCO24 to SJ).

We thank M. Komatsu (conditional *Atg7* mice) and Z. Yue (*Beclin1*$^{+/}$) for mice and T. Yoshimori for providing the ptf-LC3 plasmid. We also thank the staff of the Genetic Perturbation Platform of the Broad Institute (formerly the RNAi Platform) particularly S. Silver and O. Alkan for assistance with execution and analysis of screen data, The Genome Core of the Whitehead Institute for assistance with the Arrayscan, A. Roberts for fluorescence-activated cell sorting (FACS) analysis, P. Chin for technical assistance, and members of the White and Sabatini laboratories for helpful discussions.

Abbreviations

DCFDA	2′,7′-dichlorodihydrofluorescein diacetate
AMPK	5′ adenosine monophosphate-activated protein kinase
BA1	Bafilomycin A1

ESCRT	endosomal sorting complexes required for transport
F6P	fructose-6-phosphate
F1, 6BP	fructose-1,6-bisphosphate
F2, 6BP	fructose-2,6-bisphosphate
LC3	microtubule-associated protein 1 light chain 3
LIR	LC3 Interaction Region
mTOR	mammalian/mechanistic target of rapamycin
NAC	N-acetyl-cysteine
NSCLC	Non-Small Cell Lung Cancer
PFK-1	phosphofructokinase-1
PFKFB4	6-phosphofructo-2-kinase/fructose-2,6-biphosphatase 4
PPP	Pentose Phosphate Pathway
ROS	Reactive Oxygen Species
TDCLs	Tumor derived cell lines
UBA	ubiquitin binding domain

References

1. Rabinowitz JD, White E. Autophagy and metabolism. Science. 2010; 330(6009):1344–8. [PubMed: 21127245]
2. Strohecker AM, Guo JY, Karsli-Uzunbas G, Price SM, Chen GJ, Mathew R, et al. Autophagy Sustains Mitochondrial Glutamine Metabolism and Growth of BRAFV600E-Driven Lung Tumors. Cancer discovery. 2013
3. Guo JY, Karsli-Uzunbas G, Mathew R, Aisner SC, Kamphorst JJ, Strohecker AM, et al. Autophagy suppresses progression of K-ras-induced lung tumors to oncocytomas and maintains lipid homeostasis. Genes & development. 2013; 27(13):1447–61. [PubMed: 23824538]
4. Rao S, Tortola L, Perlot T, Wirnsberger G, Novatchkova M, Nitsch R, et al. A dual role for autophagy in a murine model of lung cancer. Nature communications. 2014; 5:3056.
5. Rosenfeldt MT, O'Prey J, Morton JP, Nixon C, MacKay G, Mrowinska A, et al. p53 status determines the role of autophagy in pancreatic tumour development. Nature. 2013; 504(7479):296–300. [PubMed: 24305049]
6. Wei H, Wei S, Gan B, Peng X, Zou W, Guan JL. Suppression of autophagy by FIP200 deletion inhibits mammary tumorigenesis. Genes & development. 2011; 25(14):1510–27. [PubMed: 21764854]
7. Huo Y, Cai H, Teplova I, Bowman-Colin C, Chen G, Price S, et al. Autophagy opposes p53-mediated tumor barrier to facilitate tumorigenesis in a model of PALB2-associated hereditary breast cancer. Cancer discovery. 2013
8. Guo JY, Chen HY, Mathew R, Fan J, Strohecker AM, Karsli-Uzunbas G, et al. Activated Ras requires autophagy to maintain oxidative metabolism and tumorigenesis. Genes & development. 2011; 25(5):460–70. [PubMed: 21317241]
9. Yang A, Rajeshkumar NV, Wang X, Yabuuchi S, Alexander BM, Chu GC, et al. Autophagy is critical for pancreatic tumor growth and progression in tumors with p53 alterations. Cancer discovery. 2014

10. Yang S, Wang X, Contino G, Liesa M, Sahin E, Ying H, et al. Pancreatic cancers require autophagy for tumor growth. Genes & development. 2011; 25(7):717–29. [PubMed: 21406549]
11. Karsli-Uzunbas G, Guo JY, Price S, Teng X, Laddha SV, Khor S, et al. Autophagy is Required for Glucose Homeostasis and Lung Tumor Maintenance. Cancer discovery. 2014
12. White E. Deconvoluting the context-dependent role for autophagy in cancer. Nature reviews Cancer. 2012; 12(6):401–10. [PubMed: 22534666]
13. Degenhardt K, Mathew R, Beaudoin B, Bray K, Anderson D, Chen G, et al. Autophagy promotes tumor cell survival and restricts necrosis, inflammation, and tumorigenesis. Cancer cell. 2006; 10(1):51–64. [PubMed: 16843265]
14. Karantza-Wadsworth V, Patel S, Kravchuk O, Chen G, Mathew R, Jin S, et al. Autophagy mitigates metabolic stress and genome damage in mammary tumorigenesis. Genes & development. 2007; 21(13):1621–35. [PubMed: 17606641]
15. Mathew R, Karp CM, Beaudoin B, Vuong N, Chen G, Chen HY, et al. Autophagy suppresses tumorigenesis through elimination of p62. Cell. 2009; 137(6):1062–75. [PubMed: 19524509]
16. Mathew R, Karantza-Wadsworth V, White E. Role of autophagy in cancer. Nature reviews Cancer. 2007; 7(12):961–7.
17. Takamura A, Komatsu M, Hara T, Sakamoto A, Kishi C, Waguri S, et al. Autophagy-deficient mice develop multiple liver tumors. Genes & development. 2011; 25(8):795–800. [PubMed: 21498569]
18. Komatsu M, Wang QJ, Holstein GR, Friedrich VL Jr, Iwata J, Kominami E, et al. Essential role for autophagy protein Atg7 in the maintenance of axonal homeostasis and the prevention of axonal degeneration. Proceedings of the National Academy of Sciences of the United States of America. 2007; 104(36):14489–94. [PubMed: 17726112]
19. Rubinsztein DC, Marino G, Kroemer G. Autophagy and aging. Cell. 2011; 146(5):682–95. [PubMed: 21884931]
20. Masiero E, Agatea L, Mammucari C, Blaauw B, Loro E, Komatsu M, et al. Autophagy is required to maintain muscle mass. Cell metabolism. 2009; 10(6):507–15. [PubMed: 19945408]
21. Sandri M, Coletto L, Grumati P, Bonaldo P. Misregulation of autophagy and protein degradation systems in myopathies and muscular dystrophies. Journal of cell science. 2013; 126(Pt 23):5325–33. [PubMed: 24293330]
22. Grumati P, Coletto L, Sabatelli P, Cescon M, Angelin A, Bertaggia E, et al. Autophagy is defective in collagen VI muscular dystrophies, and its reactivation rescues myofiber degeneration. Nature medicine. 2010; 16(11):1313–20.
23. Bernardi P, Bonaldo P. Mitochondrial dysfunction and defective autophagy in the pathogenesis of collagen VI muscular dystrophies. Cold Spring Harbor perspectives in biology. 2013; 5(5):a011387. [PubMed: 23580791]
24. Shanmugam M, McBrayer SK, Qian J, Raikoff K, Avram MJ, Singhal S, et al. Targeting glucose consumption and autophagy in myeloma with the novel nucleoside analogue 8-aminoadenosine. The Journal of biological chemistry. 2009; 284(39):26816–30. [PubMed: 19648108]
25. Hoang B, Benavides A, Shi Y, Frost P, Lichtenstein A. Effect of autophagy on multiple myeloma cell viability. Molecular cancer therapeutics. 2009; 8(7):1974–84. [PubMed: 19509276]
26. Ding WX, Ni HM, Gao W, Chen X, Kang JH, Stolz DB, et al. Oncogenic transformation confers a selective susceptibility to the combined suppression of the proteasome and autophagy. Molecular cancer therapeutics. 2009; 8(7):2036–45. [PubMed: 19584239]
27. Bellodi C, Lidonnici MR, Hamilton A, Helgason GV, Soliera AR, Ronchetti M, et al. Targeting autophagy potentiates tyrosine kinase inhibitor-induced cell death in Philadelphia chromosome-positive cells, including primary CML stem cells. The Journal of clinical investigation. 2009; 119(5):1109–23. [PubMed: 19363292]
28. Maclean KH, Dorsey FC, Cleveland JL, Kastan MB. Targeting lysosomal degradation induces p53-dependent cell death and prevents cancer in mouse models of lymphomagenesis. The Journal of clinical investigation. 2008; 118(1):79–88. [PubMed: 18097482]
29. Lu Z, Luo RZ, Lu Y, Zhang X, Yu Q, Khare S, et al. The tumor suppressor gene ARHI regulates autophagy and tumor dormancy in human ovarian cancer cells. The Journal of clinical investigation. 2008; 118(12):3917–29. [PubMed: 19033662]

30. Degtyarev M, De Maziere A, Orr C, Lin J, Lee BB, Tien JY, et al. Akt inhibition promotes autophagy and sensitizes PTEN-null tumors to lysosomotropic agents. The Journal of cell biology. 2008; 183(1):101–16. [PubMed: 18838554]
31. Amaravadi RK, Yu D, Lum JJ, Bui T, Christophorou MA, Evan GI, et al. Autophagy inhibition enhances therapy-induced apoptosis in a Myc-induced model of lymphoma. The Journal of clinical investigation. 2007; 117(2):326–36. [PubMed: 17235397]
32. Carew JS, Nawrocki ST, Kahue CN, Zhang H, Yang C, Chung L, et al. Targeting autophagy augments the anticancer activity of the histone deacetylase inhibitor SAHA to overcome Bcr-Abl-mediated drug resistance. Blood. 2007; 110(1):313–22. [PubMed: 17363733]
33. Amaravadi RK, Lippincott-Schwartz J, Yin XM, Weiss WA, Takebe N, Timmer W, et al. Principles and current strategies for targeting autophagy for cancer treatment. Clinical cancer research : an official journal of the American Association for Cancer Research. 2011; 17(4):654–66. [PubMed: 21325294]
34. White E, DiPaola RS. The double-edged sword of autophagy modulation in cancer. Clinical cancer research : an official journal of the American Association for Cancer Research. 2009; 15(17): 5308–16. [PubMed: 19706824]
35. Barnard RA, Wittenburg LA, Amaravadi RK, Gustafson DL, Thorburn A, Thamm DH. Phase I clinical trial and pharmacodynamic evaluation of combination hydroxychloroquine and doxorubicin treatment in pet dogs treated for spontaneously occurring lymphoma. Autophagy. 2014; 10(8)
36. Rangwala R, Chang YC, Hu J, Algazy K, Evans T, Fecher L, et al. Combined MTOR and autophagy inhibition: Phase I trial of hydroxychloroquine and temsirolimus in patients with advanced solid tumors and melanoma. Autophagy. 2014; 10(8)
37. Rangwala R, Leone R, Chang YC, Fecher L, Schuchter L, Kramer A, et al. Phase I trial of hydroxychloroquine with dose-intense temozolomide in patients with advanced solid tumors and melanoma. Autophagy. 2014; 10(8)
38. Rosenfeld MR, Ye X, Supko JG, Desideri S, Grossman SA, Brem S, et al. A phase I/II trial of hydroxychloroquine in conjunction with radiation therapy and concurrent and adjuvant temozolomide in patients with newly diagnosed glioblastoma multiforme. Autophagy. 2014; 10(8)
39. Vogl DT, Stadtmauer EA, Tan KS, Heitjan DF, Davis LE, Pontiggia L, et al. Combined autophagy and proteasome inhibition: A phase 1 trial of hydroxychloroquine and bortezomib in patients with relapsed/refractory myeloma. Autophagy. 2014; 10(8)
40. Mahalingam D, Mita M, Sarantopoulos J, Wood L, Amaravadi R, Davis LE, et al. Combined autophagy and HDAC inhibition: A phase I safety, tolerability, pharmacokinetic, and pharmacodynamic analysis of hydroxychloroquine in combination with the HDAC inhibitor vorinostat in patients with advanced solid tumors. Autophagy. 2014; 10(8)
41. Cheong H, Lu C, Lindsten T, Thompson CB. Therapeutic targets in cancer cell metabolism and autophagy. Nature biotechnology. 2012; 30(7):671–8.
42. Bjorkoy G, Lamark T, Brech A, Outzen H, Perander M, Overvatn A, et al. p62/SQSTM1 forms protein aggregates degraded by autophagy and has a protective effect on huntingtin-induced cell death. The Journal of cell biology. 2005; 171(4):603–14. [PubMed: 16286508]
43. Lamark T, Kirkin V, Dikic I, Johansen T. NBR1 and p62 as cargo receptors for selective autophagy of ubiquitinated targets. Cell Cycle. 2009; 8(13):1986–90. [PubMed: 19502794]
44. Pankiv S, Clausen TH, Lamark T, Brech A, Bruun JA, Outzen H, et al. p62/SQSTM1 binds directly to Atg8/LC3 to facilitate degradation of ubiquitinated protein aggregates by autophagy. The Journal of biological chemistry. 2007; 282(33):24131–45. [PubMed: 17580304]
45. Sanchez P, De Carcer G, Sandoval IV, Moscat J, Diaz-Meco MT. Localization of atypical protein kinase C isoforms into lysosome-targeted endosomes through interaction with p62. Molecular and cellular biology. 1998; 18(5):3069–80. [PubMed: 9566925]
46. Duran A, Linares JF, Galvez AS, Wikenheiser K, Flores JM, Diaz-Meco MT, et al. The signaling adaptor p62 is an important NF-kappaB mediator in tumorigenesis. Cancer cell. 2008; 13(4):343–54. [PubMed: 18394557]
47. Wooten MW, Geetha T, Seibenhener ML, Babu JR, Diaz-Meco MT, Moscat J. The p62 scaffold regulates nerve growth factor-induced NF-kappaB activation by influencing TRAF6

polyubiquitination. The Journal of biological chemistry. 2005; 280(42):35625–9. [PubMed: 16079148]

48. Komatsu M, Waguri S, Koike M, Sou YS, Ueno T, Hara T, et al. Homeostatic levels of p62 control cytoplasmic inclusion body formation in autophagy-deficient mice. Cell. 2007; 131(6):1149–63. [PubMed: 18083104]
49. Li L, Shen C, Nakamura E, Ando K, Signoretti S, Beroukhim R, et al. SQSTM1 is a pathogenic target of 5q copy number gains in kidney cancer. Cancer cell. 2013; 24(6):738–50. [PubMed: 24332042]
50. Rodriguez A, Duran A, Selloum M, Champy MF, Diez-Guerra FJ, Flores JM, et al. Mature-onset obesity and insulin resistance in mice deficient in the signaling adapter p62. Cell metabolism. 2006; 3(3):211–22. [PubMed: 16517408]
51. Duran A, Amanchy R, Linares JF, Joshi J, Abu-Baker S, Porollo A, et al. p62 is a key regulator of nutrient sensing in the mTORC1 pathway. Molecular cell. 2011; 44(1):134–46. [PubMed: 21981924]
52. Linares JF, Duran A, Yajima T, Pasparakis M, Moscat J, Diaz-Meco MT. K63 polyubiquitination and activation of mTOR by the p62-TRAF6 complex in nutrient-activated cells. Molecular cell. 2013; 51(3):283–96. [PubMed: 23911927]
53. Yalcin A, Telang S, Clem B, Chesney J. Regulation of glucose metabolism by 6-phosphofructo-2-kinase/fructose-2,6-bisphosphatases in cancer. Experimental and molecular pathology. 2009; 86(3):174–9. [PubMed: 19454274]
54. Okar DA, Lange AJ. Fructose-2,6-bisphosphate and control of carbohydrate metabolism in eukaryotes. BioFactors. 1999; 10(1):1–14. [PubMed: 10475585]
55. Okar DA, Manzano A, Navarro-Sabate A, Riera L, Bartrons R, Lange AJ. PFK-2/FBPase-2: maker and breaker of the essential biofactor fructose-2,6-bisphosphate. Trends in biochemical sciences. 2001; 26(1):30–5. [PubMed: 11165514]
56. Lipinski MM, Hoffman G, Ng A, Zhou W, Py BF, Hsu E, et al. A genome-wide siRNA screen reveals multiple mTORC1 independent signaling pathways regulating autophagy under normal nutritional conditions. Developmental cell. 2010; 18(6):1041–52. [PubMed: 20627085]
57. Chan EY, Kir S, Tooze SA. siRNA screening of the kinome identifies ULK1 as a multidomain modulator of autophagy. The Journal of biological chemistry. 2007; 282(35):25464–74. [PubMed: 17595159]
58. Orvedahl A, Sumpter R Jr, Xiao G, Ng A, Zou Z, Tang Y, et al. Image-based genome-wide siRNA screen identifies selective autophagy factors. Nature. 2011; 480(7375):113–7. [PubMed: 22020285]
59. Szyniarowski P, Corcelle-Termeau E, Farkas T, Hoyer-Hansen M, Nylandsted J, Kallunki T, et al. A comprehensive siRNA screen for kinases that suppress macroautophagy in optimal growth conditions. Autophagy. 2011; 7(8):892–903. [PubMed: 21508686]
60. He P, Peng Z, Luo Y, Wang L, Yu P, Deng W, et al. High-throughput functional screening for autophagy-related genes and identification of TM9SF1 as an autophagosome-inducing gene. Autophagy. 2009; 5(1):52–60. [PubMed: 19029833]
61. Sarkar S, Perlstein EO, Imarisio S, Pineau S, Cordenier A, Maglathlin RL, et al. Small molecules enhance autophagy and reduce toxicity in Huntington's disease models. Nature chemical biology. 2007; 3(6):331–8. [PubMed: 17486044]
62. Williams A, Sarkar S, Cuddon P, Ttofi EK, Saiki S, Siddiqi FH, et al. Novel targets for Huntington's disease in an mTOR-independent autophagy pathway. Nature chemical biology. 2008; 4(5):295–305. [PubMed: 18391949]
63. Criollo A, Senovilla L, Authier H, Maiuri MC, Morselli E, Vitale I, et al. The IKK complex contributes to the induction of autophagy. The EMBO journal. 2010; 29(3):619–31. [PubMed: 19959994]
64. McKnight NC, Jefferies HB, Alemu EA, Saunders RE, Howell M, Johansen T, et al. Genome-wide siRNA screen reveals amino acid starvation-induced autophagy requires SCOC and WAC. The EMBO journal. 2012; 31(8):1931–46. [PubMed: 22354037]

65. Luo B, Cheung HW, Subramanian A, Sharifnia T, Okamoto M, Yang X, et al. Highly parallel identification of essential genes in cancer cells. Proceedings of the National Academy of Sciences of the United States of America. 2008; 105(51):20380–5. [PubMed: 19091943]

66. Mi H, Muruganujan A, Casagrande JT, Thomas PD. Large-scale gene function analysis with the PANTHER classification system. Nature protocols. 2013; 8(8):1551–66. [PubMed: 23868073]

67. Hoyer-Hansen M, Bastholm L, Szyniarowski P, Campanella M, Szabadkai G, Farkas T, et al. Control of macroautophagy by calcium, calmodulin-dependent kinase kinase-beta, and Bcl-2. Molecular cell. 2007; 25(2):193–205. [PubMed: 17244528]

68. Law BY, Wang M, Ma DL, Al-Mousa F, Michelangeli F, Cheng SH, et al. Alisol B, a novel inhibitor of the sarcoplasmic/endoplasmic reticulum Ca(2+) ATPase pump, induces autophagy, endoplasmic reticulum stress, and apoptosis. Molecular cancer therapeutics. 2010; 9(3):718–30. [PubMed: 20197400]

69. Rusten TE, Stenmark H. How do ESCRT proteins control autophagy? Journal of cell science. 2009; 122(Pt 13):2179–83. [PubMed: 19535733]

70. Rusten TE, Vaccari T, Stenmark H. Shaping development with ESCRTs. Nature cell biology. 2012; 14(1):38–45. [PubMed: 22193162]

71. Tamai K, Tanaka N, Nara A, Yamamoto A, Nakagawa I, Yoshimori T, et al. Role of Hrs in maturation of autophagosomes in mammalian cells. Biochemical and biophysical research communications. 2007; 360(4):721–7. [PubMed: 17624298]

72. Li L, Guan KL. Microtubule-associated protein/microtubule affinity-regulating kinase 4 (MARK4) is a negative regulator of the mammalian target of rapamycin complex 1 (mTORC1). The Journal of biological chemistry. 2013; 288(1):703–8. [PubMed: 23184942]

73. Qin Q, Inatome R, Hotta A, Kojima M, Yamamura H, Hirai H, et al. A novel GTPase, CRAG, mediates promyelocytic leukemia protein-associated nuclear body formation and degradation of expanded polyglutamine protein. The Journal of cell biology. 2006; 172(4):497–504. [PubMed: 16461359]

74. Fallon L, Moreau F, Croft BG, Labib N, Gu WJ, Fon EA. Parkin and CASK/LIN-2 associate via a PDZ-mediated interaction and are co-localized in lipid rafts and postsynaptic densities in brain. The Journal of biological chemistry. 2002; 277(1):486–91. [PubMed: 11679592]

75. Jager S, Bucci C, Tanida I, Ueno T, Kominami E, Saftig P, et al. Role for Rab7 in maturation of late autophagic vacuoles. Journal of cell science. 2004; 117(Pt 20):4837–48. [PubMed: 15340014]

76. Gutierrez MG, Munafo DB, Beron W, Colombo MI. Rab7 is required for the normal progression of the autophagic pathway in mammalian cells. Journal of cell science. 2004; 117(Pt 13):2687–97. [PubMed: 15138286]

77. Ganley IG, Wong PM, Gammoh N, Jiang X. Distinct autophagosomal-lysosomal fusion mechanism revealed by thapsigargin-induced autophagy arrest. Molecular cell. 2011; 42(6):731–43. [PubMed: 21700220]

78. Ros S, Santos CR, Moco S, Baenke F, Kelly G, Howell M, et al. Functional metabolic screen identifies 6-phosphofructo-2-kinase/fructose-2,6-biphosphatase 4 as an important regulator of prostate cancer cell survival. Cancer discovery. 2012; 2(4):328–43. [PubMed: 22576210]

79. Ros S, Schulze A. Balancing glycolytic flux: the role of 6-phosphofructo-2-kinase/fructose 2,6-bisphosphatases in cancer metabolism. Cancer & metabolism. 2013; 1(1):8. [PubMed: 24280138]

80. Minchenko OH, Ochiai A, Opentanova IL, Ogura T, Minchenko DO, Caro J, et al. Overexpression of 6-phosphofructo-2-kinase/fructose-2,6-bisphosphatase-4 in the human breast and colon malignant tumors. Biochimie. 2005; 87(11):1005–10. [PubMed: 15925437]

81. Warmoes MO, Locasale JW. Heterogeneity of glycolysis in cancers and therapeutic opportunities. Biochemical pharmacology. 2014; 92(1):12–21. [PubMed: 25093285]

82. Jeon YK, Yoo DR, Jang YH, Jang SY, Nam MJ. Sulforaphane induces apoptosis in human hepatic cancer cells through inhibition of 6-phosphofructo-2-kinase/fructose-2,6-biphosphatase4, mediated by hypoxia inducible factor-1-dependent pathway. Biochimica et biophysica acta. 2011; 1814(10): 1340–8. [PubMed: 21640852]

83. Goidts V, Bageritz J, Puccio L, Nakata S, Zapatka M, Barbus S, et al. RNAi screening in glioma stem-like cells identifies PFKFB4 as a key molecule important for cancer cell survival. Oncogene. 2012; 31(27):3235–43. [PubMed: 22056879]

84. Kimura S, Noda T, Yoshimori T. Dissection of the autophagosome maturation process by a novel reporter protein, tandem fluorescent-tagged LC3. Autophagy. 2007; 3(5):452–60. [PubMed: 17534139]
85. Mizushima N, Yoshimori T, Levine B. Methods in mammalian autophagy research. Cell. 2010; 140(3):313–26. [PubMed: 20144757]
86. Yoshimori T, Yamamoto A, Moriyama Y, Futai M, Tashiro Y. Bafilomycin A1, a specific inhibitor of vacuolar-type H(+)-ATPase, inhibits acidification and protein degradation in lysosomes of cultured cells. The Journal of biological chemistry. 1991; 266(26):17707–12. [PubMed: 1832676]
87. Zhou R, Yazdi AS, Menu P, Tschopp J. A role for mitochondria in NLRP3 inflammasome activation. Nature. 2011; 469(7329):221–5. [PubMed: 21124315]
88. Scherz-Shouval R, Shvets E, Fass E, Shorer H, Gil L, Elazar Z. Reactive oxygen species are essential for autophagy and specifically regulate the activity of Atg4. The EMBO journal. 2007; 26(7):1749–60. [PubMed: 17347651]
89. Chen Y, Azad MB, Gibson SB. Superoxide is the major reactive oxygen species regulating autophagy. Cell death and differentiation. 2009; 16(7):1040–52. [PubMed: 19407826]
90. Lee J, Giordano S, Zhang J. Autophagy, mitochondria and oxidative stress: cross-talk and redox signalling. The Biochemical journal. 2012; 441(2):523–40. [PubMed: 22187934]
91. Jain A, Lamark T, Sjottem E, Larsen KB, Awuh JA, Overvatn A, et al. p62/SQSTM1 is a target gene for transcription factor NRF2 and creates a positive feedback loop by inducing antioxidant response element-driven gene transcription. The Journal of biological chemistry. 2010; 285(29): 22576–91. [PubMed: 20452972]
92. Sahani MH, Itakura E, Mizushima N. Expression of the autophagy substrate SQSTM1/p62 is restored during prolonged starvation depending on transcriptional upregulation and autophagy-derived amino acids. Autophagy. 2014; 10(3):431–41. [PubMed: 24394643]
93. Yang Z, Goronzy JJ, Weyand CM. The glycolytic enzyme PFKFB3/phosphofructokinase regulates autophagy. Autophagy. 2014; 10(2):382–3. [PubMed: 24351650]
94. Yang Z, Fujii H, Mohan SV, Goronzy JJ, Weyand CM. Phosphofructokinase deficiency impairs ATP generation, autophagy, and redox balance in rheumatoid arthritis T cells. The Journal of experimental medicine. 2013; 210(10):2119–34. [PubMed: 24043759]
95. Klarer AC, O'Neal J, Imbert-Fernandez Y, Clem A, Ellis SR, Clark J, et al. Inhibition of 6-phosphofructo-2-kinase (PFKFB3) induces autophagy as a survival mechanism. Cancer & metabolism. 2014; 2(1):2. [PubMed: 24451478]
96. Bensaad K, Cheung EC, Vousden KH. Modulation of intracellular ROS levels by TIGAR controls autophagy. The EMBO journal. 2009; 28(19):3015–26. [PubMed: 19713938]
97. Bensaad K, Tsuruta A, Selak MA, Vidal MN, Nakano K, Bartrons R, et al. TIGAR, a p53-inducible regulator of glycolysis and apoptosis. Cell. 2006; 126(1):107–20. [PubMed: 16839880]

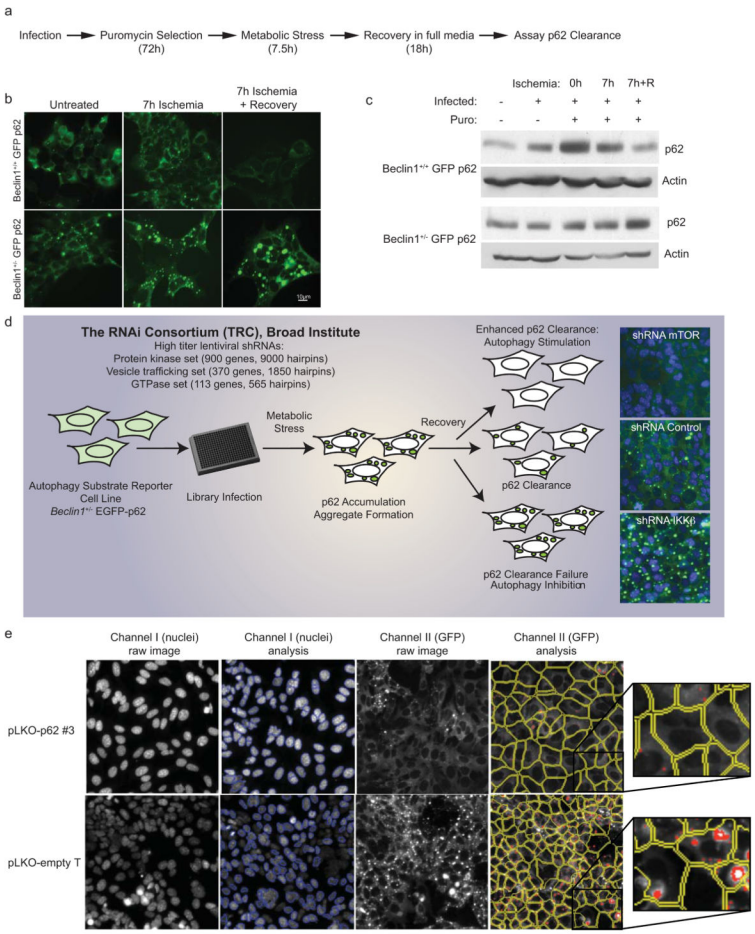

Figure 1. Identification of Autophagy Substrate Modulators by High Content shRNA Screening

a. Experimental timeline detailing sequence of infection, selection, and assay for p62 elimination.

b. *Beclin1*$^{+/+}$ or *Beclin1*$^{+/-}$ iBMK cells stably expressing EGFP-p62 were infected with shRNA targeting Luc1510, selected with puromycin, and subjected to a time course of 7 hours ischemia and recovery. Representative images of GFP-p62 accumulation during stress and recovery demonstrating impaired elimination of p62 from the *Beclin1*$^{+/-}$ iBMK cell line during recovery in full media. Scale bar is 10 μm.

c. Western blot analysis of GFP-p62 accumulation and elimination in *Beclin1*$^{+/+}$ or *Beclin1*$^{+/-}$ iBMK cells stably expressing EGFP-p62 infected with shRNA targeting Luc1510, selected with puromycin, and subjected to a time course of 7 hours ischemia and recovery as indicated.

d. Schematic representation of the p62 modulator screen. Representative images from the screen are provided for each class of regulator.

e. A customized Cellomics algorithm was used to score p62 abundance at the single cell level. Images from pilot studies employing p62 or non-targeting (emptyT) hairpins are provided with and without the overlaid analysis. Cells were counterstained with Hoechst 33342 to visualize nuclei (blue, Channel 1). Channel 2 maps the cell borders, and detects GFP-p62 levels within a designated radius from the nucleus (Ring Spot Total Intensity). 9

images per field were collected to ensure representative coverage. A p62 aggregate score equal to Mean Ring Spot total intensity/Mean nuclei was calculated for each well.

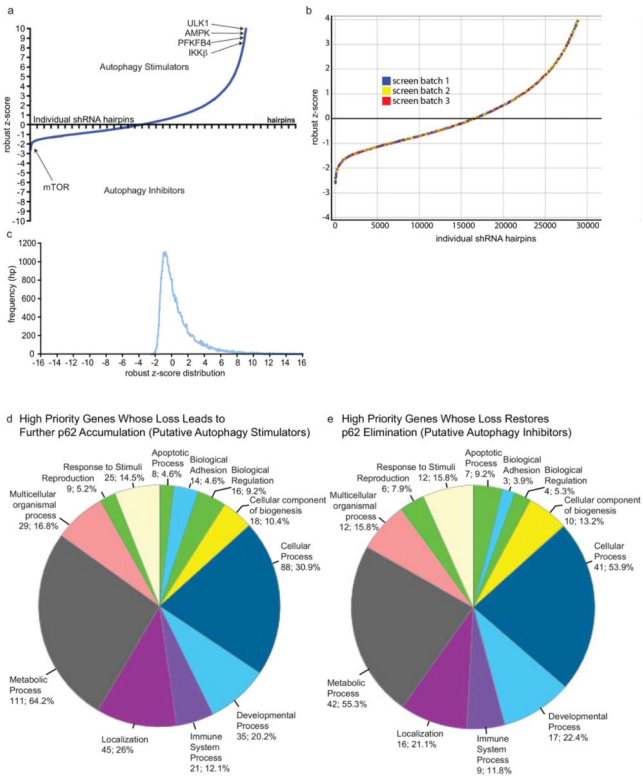

Figure 2. Screen Performance and Analytics

a. Distribution of all hairpins in the screen after filtering to remove hairpins with poor infection efficacy and wells containing less than 1500 nuclei, likely representing autofocus errors, plotted against robust-z-score. The location known positive (ULK1, AMPK, IKKβ) and negative regulators of the autophagy pathway (mTOR) is shown.

b. Overlay of hairpin distribution for all three of the screen batches demonstrating little to no batch-to-batch variation in the data.

c. Histogram of hairpin frequency plotted against robust z-score

d–e. Classification of autophagy screen hits arranged by Biological Process by the PANTHER system. # genes in the screen dataset found within each category; % of genes in the data set contained within each category.

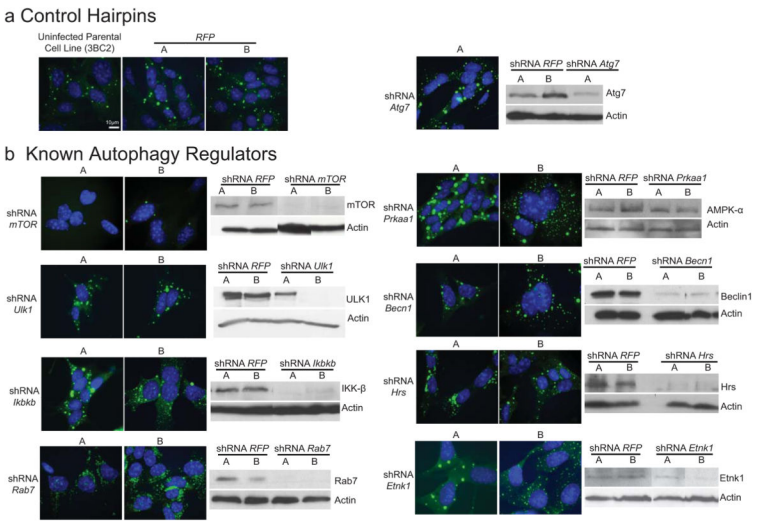

Figure 3. Validation of Selected Screen Hits

a. Representative low throughput validation images from experiments with uninfected parental *Beclin1*$^{+/-}$ iBMK cells (3BC2-clone #D3) or *Beclin1*$^{+/-}$ iBMK cells infected with two distinct hairpins targeting red fluorescent protein (*RFP*) or a hairpin targeting *Atg7*, assaying GFP-p62 clearance following metabolic stress (7.5h) and recovery (18h) in full media. Nuclei were counterstained with Hoechst 33342 to facilitate visualization. Scale bar is 10 μm. Non-validating hairpins were spliced out of the western blots presented for aesthetic reasons. All lanes presented for a given gene were contained within a single gel. Complete gels are shown in Figure S1.

b. Validation of a subset of known autophagy regulators identified in our screens. For a candidate gene to pass validation at least two individual hairpins targeting distinct regions of the message must silence expression of the target gene by western blot and correlate well with GFP-p62 phenotype observed microscopically. *Beclin1*$^{+/-}$ iBMK cells were infected with hairpins targeting red fluorescent protein (*RFP*) or *mTOR*, *Ulk1*, *Prkaa1*, *Becn1*, *Ikbkb*, *Hrs*, *Rab7*, or *Etnk1*, subjected to selection, and assayed for GFP-p62 clearance following metabolic stress (7.5h) and recovery (18h) in full media by immunofluoresence. Nuclei were counterstained with Hoechst 33342 to facilitate visualization. Scale bar is 10 μm. Confirmation of on-target gene silencing was obtained by western blot analysis. TRC hairpin identifiers and antibody details are contained in the Supplemental Methods section. Non-validating hairpins were spliced out of the western blots presented for aesthetic reasons. All lanes presented for a given gene were contained within a single gel. Complete gels are shown in Figure S1.

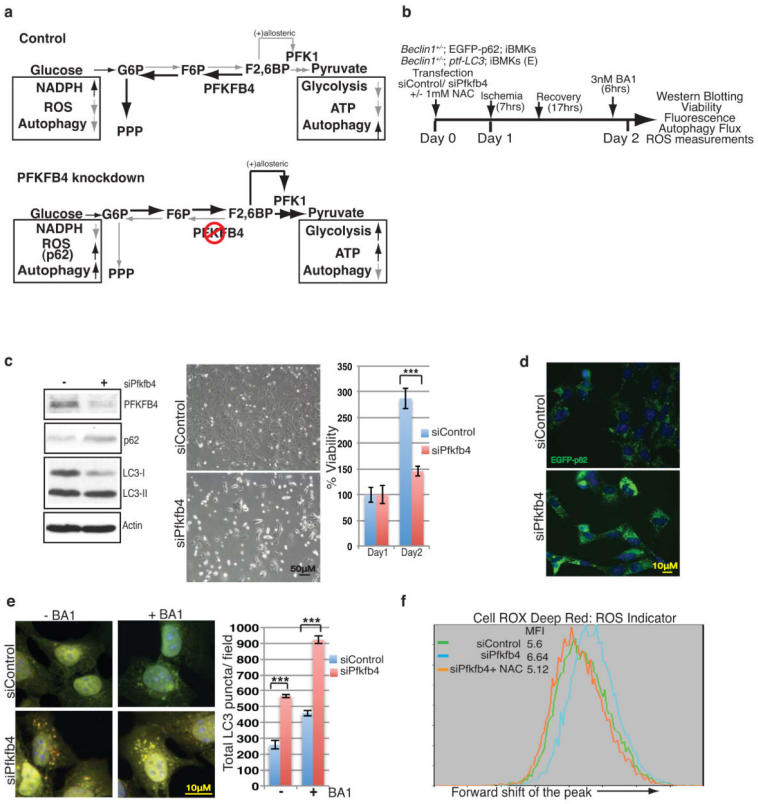

Figure 4. Validation of PFKFB4 as an Autophagy Regulator in *Beclin1*$^{+/-}$; EGFP-p62 iBMKs

a. Proposed mechanism of action of autophagy modulation by PFKFB4

b. Experimental timeline for assessment of PFKFB4-mediated autophagic regulation in the iBMK system.

c. Western blot analysis of PFKFB4, LC3, and p62 expression in *Beclin1*$^{+/-}$; EGFP-p62 iBMKs, 2 days post-transfection with siControl or siPfkfb4. Actin is used as loading control. Representative phase contrast images and viability graphs of *Beclin1*$^{+/-}$; EGFP-p62 iBMKs 2 days post-transfection with siControl or siPfkfb4. Error bars represent ± standard deviation (***$p < 0.0001$). Scale bar is 50 μm.

d. Representative fluorescence images showing EGFP-p62 accumulation in *Beclin1*$^{+/-}$; EGFP-p62 iBMKs, 2 days post-transfection with siPfkfb4. Scale bar is 10 μm.

e. Autophagy flux analysis of *Beclin1*$^{+/-}$; iBMKs stably expressing ptf-LC3 in absence and presence of 3nM BA1 2 days post-transfection with siControl or siPfkfb4. Representative fluorescence images and corresponding quantitation are provided. Error bars represent ± standard deviation (***$p < 0.0001$). Scale bar is 10 μm.

f. Cell ROX analysis of ROS levels, 2 days post-transfection in the presence or absence of 1mM NAC. Representative histograms are provided.

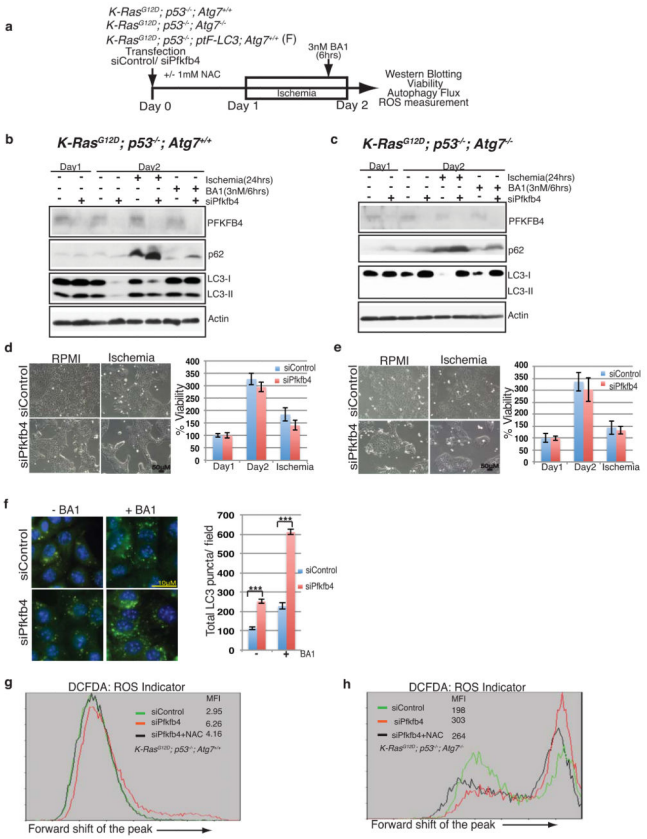

Figure 5. PFKFB4 Functions as an Autophagy Inhibitor in K-Ras-driven TDCLs

a. Experimental timeline for assessment of PFKFB4-mediated autophagic regulation in K-Ras-driven TDCLs.

b–c. Western blot analysis of PFKFB4, p62, and LC3 in *K-Ras*$^{G12D/+}$; *p53*$^{-/-}$; *Atg7*$^{+/+}$(b) and *K-Ras*$^{G12D/+}$; *p53*$^{-/-}$; *Atg7*$^{-/-}$ (c) cell lines grown in normal media conditions or subjected to 24h ischemia, 1 and 2 days post-transfection with siControl or siPfkfb4. Cells were incubated in the presence or absence of 3nM BA1 as indicated.

d–e. Representative phase contrast images and associated viability graphs of autophagy competent *K-Ras*$^{G12D/+}$; *p53*$^{-/-}$; *Atg7*$^{+/+}$ (d) and autophagy deficient *K-Ras*$^{G12D/+}$; *p53*$^{-/-}$; *Atg7*$^{-/-}$ (e) cells in normal media or ischemic conditions, 2 days post-transfection with siControl or siPfkfb4. Scale bar is 50 μm.

f. Autophagy flux analysis of *K-Ras*$^{G12D/+}$; *p53*$^{-/-}$; *Atg7*$^{+/+}$ stably expressing ptf-LC3 in absence and presence of 3nM BA1, 2 days post-transfection with siControl or siPfkfb4. Representative fluorescence images and corresponding quantitation are provided. Error bars represent ± standard deviation (***p < 0.0001). Scale bar is 10 μm.

g–h. DCFDA analysis of ROS levels in *K-Ras*$^{G12D/+}$; *p53*$^{-/-}$; *Atg7*$^{+/+}$ (g) and *K-Ras*$^{G12D/+}$; *p53*$^{-/-}$; *Atg7*$^{-/-}$ (h) 2 days post-transfection with siPfkfb4 in the presence or absence of 1mM NAC. Representative histograms are provided.

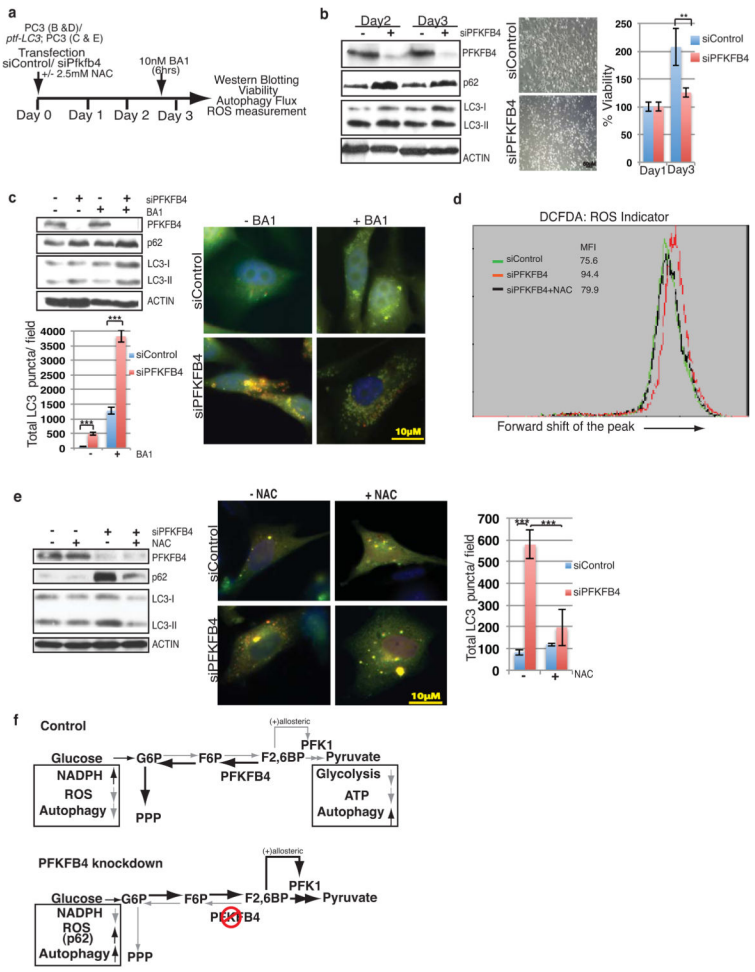

Figure 6. PFKFB4 Mitigates ROS to Suppress Autophagy and p62 Accumulation in PC3 Cells

a. Experimental timeline for assessment of PFKFB4-mediated autophagy regulation in PC3 cells.

b. Western blot analysis of PFKFB4, p62 and LC3 in PC3 cells, 2 and 3 days post-transfection with siControl or siPFKFB4. Representative phase contrast images and viability graphs of PC3 cells 3 days post-transfection with siControl or siPFKFB4 are provided. Error bars represent ± standard deviation (**$p < 0.005$). Scale bar is 50 μm.

c. Autophagy flux analysis of PC3 cells stably expressing ptf-LC3, 3 days post-transfection with siControl or siPFKFB4 in the presence or absence of BA1. Representative western blots of PFKFB4, p62, LC3, fluorescence images and corresponding quantitation are provided. Scale bar is 10 μm.

d. DCFDA analysis of ROS levels in PC3 cells 3 days post-transfection with siControl or siPFKFB4 in the presence or absence of 2.5mM NAC as indicated. Representative histograms are provided.

e. Autophagy flux analysis of PC3 cells stably expressing ptf-LC3 3 days post-transfection with siControl or siPFKFB4, in the presence or absence 2.5mM NAC. Representative western blots of PFKFB4, p62, LC3, fluorescence images and quantitation graph are

provided. Error bars represent ± standard deviation (S.D.). (***$p < 0.0001$). Scale bar is 10 μm.

f. Model of PFKFB4 mediated regulation of autophagy by controlling redox balance of the cell.

Oncogene. Author manuscript; available in PMC 2016 May 05.

Table 1

Positive Regulators of Autophagy

Genes Whose Loss Leads to Further p62 Accumulation.

Symbol	Gene ID	Symbol	Gene ID	Symbol	Gene ID	Symbol	Gene ID
2810408M09Rik	66566	Epha6	13840	Nkiras2	71966	Rragc	54170
Acvr2a	11480	Epha7	13841	Nme2	18103	Rras2	66922
Acvr2b	11481	Ephb6	13848	Nme7	171567	Ryk	20187
Adrbk2	320129	Etnk1	75320	Ntpcr	66566	Sbk3	381835
Agap3	213990	Etnk2	214253	Nuak1	77976	Sec23a	20334
Ak2	11637	Fastkd5	380601	Pak4	70584	Septin11	52398
Aldh18a1	56454	Fgfr4	14186	Pank3	211347	Sh3gl2	20404
Ankk1	244859	Gbp3	55932	Pdgfrl	68797	Shpk	74637
Anxa7	11750	Gck	103988	Pdpk1	18607	Sik1	17691
Ap1g1	11765	Gm318	545204	Pfkfb3	170768	Smg1	233789
Ap1s1	11769	Gm4776	212225	Pfkfb4	270198	Smok2a	27263
Ap3m2	64933	Gm4862	229879	Pftk1	18647	Smok4a	272667
Araf	11836	Gm5285	383956	Phka1	18679	Snap29	67474
Arf5	11844	Gm5374	385049	Phkg1	18682	Snx13	217463
Arfrp1	76688	Gm5425	432482	Phkg2	68961	Snx16	74718
Arl4d	80981	Gm9824	432447	Pi4ka	224020	Snx2	67804
Arpc1a	56443	Golga5	27277	Pik3c2a	18704	Snx3	54198
Arpc2	76709	Gpn1	74254	Pik3cg	30955	Snx4	69150
B2m	12010	Grk6	26385	Pkmyt1	268930	Stk22d	117545
Becn1	56208	Gsg2	14841	Plaur	18793	Stk35	67333
Camk1g	215303	Gtpbp2	56055	Prkaa1	105787	Stradb	227154
Camk2g	12325	Gtpbp4	69237	Prkaa2	108079	Stx16	228960
Camk4	12326	Gucy2e	14919	Prkag1	19082	Synj2	20975
Camkk1	55984	H2bfm	69389	Prkar2b	19088	Syt15	319508
Cav3	12391	Hgs	15239	Prkcd	18753	Syt8	55925
Cdadc1	71891	Hipk2	15258	Prkcdbp	109042	Tesk2	230661
Cdc2l1	12537	Hras1	15461	Prkcz2	404705	Tie1	21846

Symbol	Gene ID	Symbol	Gene ID	Symbol	Gene ID	Symbol	Gene ID
Cdc42bpg	240505	Hspb8	80888	Prps1l1	75456	Tjp2	21873
Cdk3	69681	Ikbkb	16150	Psmc1	19179	Trp53rk	76367
Cdkl5	382253	Irak1	16179	Rab14	68365	Trpm6	225997
Cerk	223753	Irak3	73914	Rab15	104886	Tspan6	56496
Chek1	12649	Itpka	228550	Rab19	19331	Tspan7	21912
Chmp4b	75608	Keap1	50868	Rab20	19332	Tssk3	58864
Chmp5	76959	Khk	16548	Rab3d	19340	Txk	22165
Ciita	12265	Kpnb1	16211	Rab6b	270192	Uck1	22245
Ckmt2	76722	Map2k3	26397	Rab7	19349	Uck2	80914
Csnk1g1	214897	Map3k14	53859	Rab8a	17274	Ulk1	22241
Cyth3	13132	Mapk9	26420	Rac1	19353	Vps13a	271564
Dab2	217480	Mapkapk3	102626	Rac3	170758	Vps36	70160
Dgkb	217480	Mark4	232944	Rap1a	109905	Vps39	269338
Dlg4	13385	Mast3	546071	Rasl10b	276952	Vps4b	20479
Dnm2	13430	Mknk2	17347	Rerg	232441	Vps8	209018
Doc2b	13447	Mlkl	74568	Rhoc	11853	Vti1b	53612
Drg2	13495	Mst1r	19882	Rhog	56212	Wnk4	69847
Eef1a2	13628	Mylk4	238564	Rhot1	59040	Yes1	22612
Eif2s3y	26908	N4bp2	333789	Rhov	228543		
Epha5	13839	Nkiras1	69721	Rps6kl1	238323		

Table 2

Negative Regulators of Autophagy

Genes Whose Loss Restores p62 Elimination.

Symbol	Gene ID	Symbol	Gene ID	Symbol	Gene ID	Symbol	Gene ID
1810024B03Rik	329509	Dlg4	13385	Mtor	56717	Ripk3	56532
4932415M13Rik	211496	Egfr	13649	Musk	18198	Sar1a	20224
Adk	11534	Eif2ak1	15467	N4bp2	333789	Scfd1	76983
Akt1	11651	Ephb1	270190	Nek5	330721	Snx10	71982
Alpk3	116904	Ern1	78943	Pfkfb4	270198	Stxbp3a	20912
Arf3	11842	Gm14147	381390	Pik3c3	225326	Sybu	319613
Arhgap24	231532	Gm4922	237300	Pldn	18457	Tlk2	24086
Atp6v0a1	11975	Gm5374	385049	Plk2	20620	Tpr	108989
Bmpr1a	12166	Grk4	14772	Prkaca	18747	Trib3	228775
Brdt	114642	Hip1	215114	Prkcz	18762	Trrap	100683
Cask	12361	Hip1r	29816	Rab34	19376	Tssk3	58864
Cdk6	12571	Kpna2	16647	Rab39b	67790	Txndc3	73412
Cdk8	264064	Lrguk	74354	Rab7l1	226422	Vamp8	22320
Chmp1a	234852	Map3k11	26403	Rab9	56382	Vapa	30960
Cpne3	70568	Map4k3	225028	Rabl2a	68708	Vps33b	233405
Ddr2	18214	Mapk14	26416	Rhoa	11848	Vta1	66201
Dgka	13139	Mpp3	13384	Rhoh	74734		